

Electrodeposition of highly ordered macroporous iridium oxide through self-assembled colloidal templates

Jin Hu,^a Mamdouh Abdelsalam,^a Philip Bartlett,^a Robin Cole,^b Yoshihiro Sugawara,^b Jeremy Baumberg,^b Sumeet Mahajan^b and Guy Denuault^{*a}

Received 8th January 2009, Accepted 20th March 2009

First published as an Advance Article on the web 24th April 2009

DOI: 10.1039/b900279k

Iridium oxide electrodeposited through a self-assembled colloidal template has an inverse opal structure. Monolayers present long range hexagonal arrangements of hemispherical nanocavities while multilayers present 3D honeycomb structures with spherical voids. The films are amorphous, have several electroactive redox states and are electrochromic. The nanostructure modifies their reflectivity thus indicating that these films could be used as tunable photonic devices.

Introduction

Iridium oxide (IrOx) films are well known for their applications in electrochromism,^{1,2} physiology^{3,4} and pH sensing.⁵⁻⁷ However, the preparation of plain IrOx films is not trivial and that of nanostructured IrOx films even more challenging. Many articles describe the preparation of IrOx nanoparticles,⁸ nanowires,^{9,10} and nanocrystals^{11,12} but very few report the preparation of nanostructured IrOx films.^{13,14} Here we describe, for the first time, the fabrication of highly ordered micrometre thick macroporous films of iridium oxide using electrodeposition through a self-assembled colloidal template. The films are grown by potentiostatic cycling in an iridium complex solution. A few cycles produce highly ordered arrays of hemispherical cups with long range hexagonal symmetry. Growth can be finely controlled *via* the cycle number and structures ranging from fully open to partially closed cups can be prepared. Further cycling yields porous films up to three template layers thick with a 3D honeycomb internal structure. Upon characterisation with X-ray diffraction, Raman spectroscopy, SEM, voltammetry, and reflectivity measurements, the films are found to be amorphous, to have structural dimensions faithful to that of the template, several electroactive redox states and reflectivity spectra significantly different from that of non-structured films. Such films should find applications in biology (IrOx is conducting, non reactive and biocompatible) but particularly optics because their optical density can be electrochemically controlled and the cavity diameters correspond to UV-visible wavelengths.

Experimental

Gold electrodes and colloidal templates were prepared and characterised as described previously.¹⁵ The IrOx deposition solution¹⁶ was prepared as follows: anhydrous IrCl₄ (0.07 g, Alfa-Aesar) was dissolved in 50 ml of water then stirred for 30 min.

^aSchool of Chemistry, University of Southampton, Highfield, Southampton, UK, SO17 1BJ. E-mail: gd@soton.ac.uk; Fax: +44 (0)23 80593781; Tel: +44 (0)23 80592154

^bNanoPhotonics Centre, Department of Physics, University of Cambridge, JJ Thomson Ave, Cambridge, UK, CB3 0HE. E-mail: j.j.baumberg@phy.cam.ac.uk; Fax: +44 (0)1223 764515; Tel: +44 (0)1223 337313

Aqueous H₂O₂ (0.5 ml, 30%, Aldrich) was added and the resulting solution was stirred for 10 min. Oxalic acid dehydrate (~250 mg, Aldrich) was added and the solution was stirred for another 10 min. The pH was slowly adjusted to 10.5 by the addition of potassium carbonate (Aldrich). The resulting yellowish brown solution was covered and left at room temperature for 3–4 d to stabilise after which it appeared deep purple. The deposition of IrOx was carried out by cyclic voltammetry between –0.8 and +0.7 V *vs.* SCE at 100 mV s⁻¹ with a PGSTAT30 (Autolab, Eco Chemie) with the cell inside a grounded Faraday cage. The template was dissolved with dimethylformamide under sonication and the films were washed in pure water. Scanning electron microscopy images were acquired with an XL30 ESEM (Philips) and a JSM 6500F (Jeol). Raman spectra were recorded on a Renishaw Raman 2000 microscope with a 633 nm HeNe laser and a 1 μm diameter spot size. Reflectivity spectra were measured with a coherent white-light source with the sample mounted on a goniometric stage.¹⁷

Results and discussion

IrOx films are produced by electrochemical oxidation of iridium electrodes,^{18,19} thermal decomposition of iridium salts,²⁰ reactive sputtering,²¹ chemical vapour deposition,¹⁴ mixing solid IrO₂ with a matrix²² or by electrodeposition from a soluble precursor.^{16,23} The latter was chosen because of our experience in the templated electrodeposition of nanostructured materials.^{24–28} Templated electrodeposition has proved to be an excellent means to tune the properties of materials by modifying their structure rather than their elemental composition. Using this method, nanostructured gold films are prepared to control surface plasmons and produce tunable photonic surfaces^{15,29–33} and to amplify surface enhanced Raman signals^{34,35} or control wetting and design hydrophobic surfaces.³⁶ Similarly nanostructured templated Ni₈₀Fe₂₀ films are prepared with different coercivities by selecting templates with different dimensions.^{37,38} In all cases, the internal geometry and the dimensions of the cavities determine the properties of the material.

The template is prepared by placing a drop of a colloidal suspension of monodisperse spheres onto a gold coated glass slide and controlling solvent evaporation to produce a deposit of

spheres. Driven by capillary forces the spheres assemble into long range, hexagonal close packed arrays³⁹ which form the mould for the electrodeposition. Adsorbing a cysteamine monolayer onto the gold substrate improves its wettability and controls its surface charge to help anchor the first layer of spheres.⁴⁰ To produce a film the substrate and its template are immersed in an electrolyte containing a precursor (a salt or a complex) and the substrate is connected to a potentiostat which drives the deposition. Growth occurs within the voids between the spheres. The spheres are removed by dissolution and the film obtained is the cast of the template. Thicknesses ranging from fractions of a template layer to several template layers can be obtained by adjusting the deposition time. Up to $\frac{1}{2}d$ where d is the sphere diameter, the film consists of a hexagonal arrangement of sphere segment cups. Beyond $\frac{1}{2}d$, the film turns into a network of interconnecting spheres and sphere segment cavities akin to a reticulated three dimensional honeycomb construction. The film structure is tailored by selecting the diameters of the spheres (typically between 100 nm and 2 μm) and the deposition time. The procedure has been used to prepare metals and alloys,^{25,38,41,42} semiconductors,⁴³ conducting polymers,^{26,44} and oxides.^{45–47}

The preparation of IrOx films followed the method reported by Yamanaka.¹⁶ Fig. 1 shows a typical set of voltammograms recorded during the deposition. In absence of a template, Fig. 1A, the voltammograms are similar to those produced by potential cycling of an iridium wire in acid.^{1,48} The larger current density observed when depositing with the template, Fig. 1B, suggests a greater efficiency, possibly because the homogeneous reaction¹⁶ which leads to the oxide deposition is confined within the voids of the template. The voltammograms are much less slanted, thus suggesting better conductivity in the structured film. The anodic and cathodic peaks have been reported to correspond to the transitions between three different oxidation states, namely Ir(III) for $E < C1$, Ir(IV) for $A1 < E < C2$ and Ir(V) for $E > A2$.²³ During the growth of templated films, the charge passed depends almost linearly on the number of voltammetric cycles, Fig. 2, and the anodic to cathodic charge ratio is equal to one at all cycle numbers. This suggests that the whole of the film is reversibly oxidised and reduced during cycling and demonstrates that cyclic voltammetry provides a fine degree of control over the amount of oxide deposited. Results are markedly different with flat films. Further voltammetric characterisation of the films in basic conditions (0.1 M Na₂CO₃, pH 10.9) (in acid the templated films have broad voltammetric peaks which are harder to analyse) produce a linear relationship between the peak currents and the scan rate therefore indicating the absence of kinetic effects over the 20–200 mV s⁻¹ range studied. Both flat and structured films were seen to change colour during potential cycling (from transparent for $E < 0.3$ V vs. SCE to dark blue for $E > 0.5$ V vs. SCE) thus indicating that the electrochromism of the IrOx films did not disappear with the templated structure.

In Fig. 3, SEM micrographs taken at different stages of deposition show the remarkable structure of the film left after removal of the template. Initially, Fig. 3A, the presence of the deposit is only confirmed by the difference in contrast between the gold substrate and IrOx, but the hexagonal symmetry is already obvious. After fewer than ten cycles the shape of the deposit appears, Fig. 3B, but the underlying granular structure of

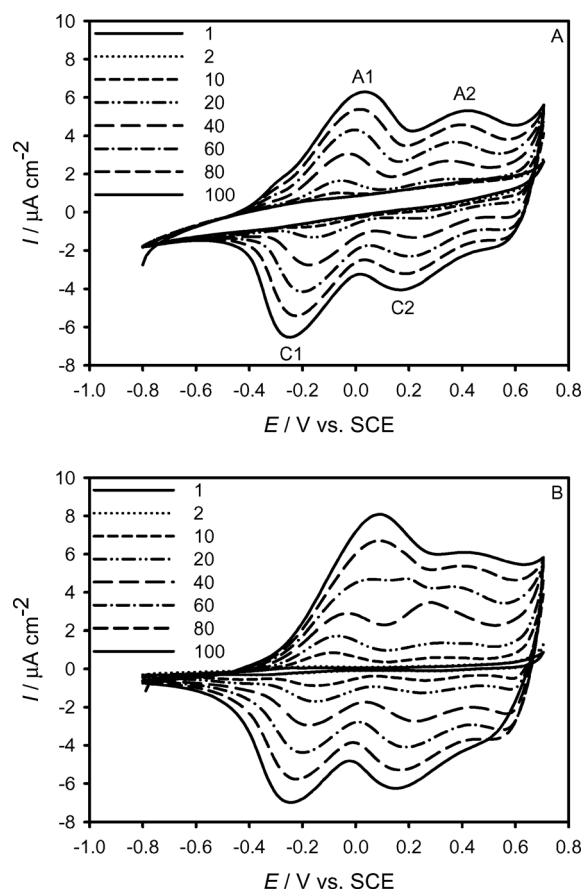


Fig. 1 Voltammograms for the growth of IrOx films on gold electrodes recorded in the deposition solution at 100 mV s⁻¹. (A) No template, (B) with a 600 nm diameter polystyrene template. Voltammetric cycle numbers are indicated against corresponding line styles. The current density was calculated using the geometric electrode area.

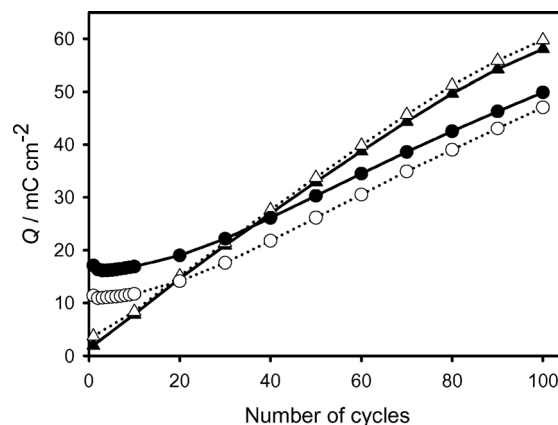


Fig. 2 Anodic (\blacktriangle , \bullet) and cathodic (\triangle , \circ) charge densities recorded during film growth for a structured film (triangles) and a flat film (circles) against the number of voltammetric cycles. Conditions were similar to Fig. 1.

the substrate is still clearly visible. When the film thickness, h , reaches a height of $\sim \frac{1}{2}d$, Fig. 3C, the smooth wall of the IrOx cups can be seen. The cup diameters follow closely that of the polystyrene spheres of the template. Except for the cup rims

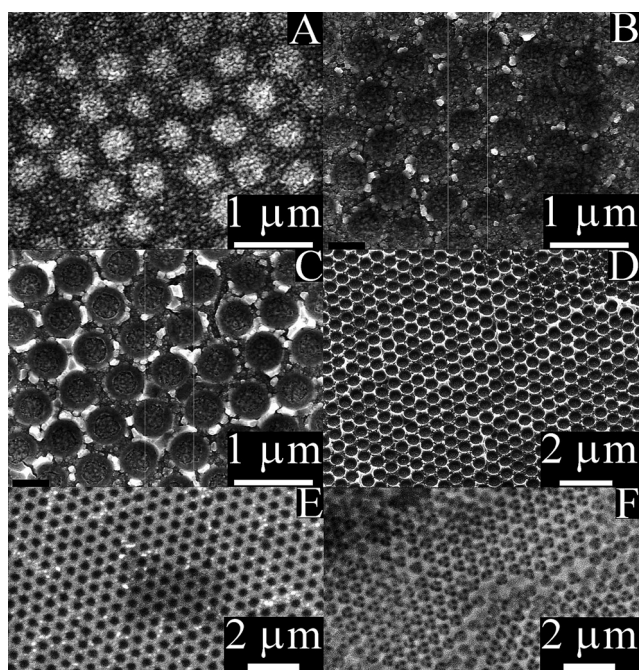


Fig. 3 Micrographs of IrOx films produced by cyclic voltammetry (same conditions as in Fig. 1) with a 600 nm diameter polystyrene template. (A) ~ 20 cycles, (B) ~ 40 cycles, $h \approx \frac{1}{2}d$, (C) ~ 60 cycles, $h \approx \frac{1}{2}d$, (D) ~ 80 cycles, (E) ~ 100 cycles, $h \approx d$, (F) ~ 200 cycles, $h > d$.

which show variations in texture, Fig. 3D, the film is uniform and free from defects over a very long range. Beyond $\frac{1}{2}d$, the cups gradually close, Fig. 3E, but again the films are virtually free of defects. Fig. 3F shows a typical film grown through several template layers; the 3D honeycomb internal structure characteristic of inverted opals is clearly visible. Up to one template layer, the film thickness measured by SEM, is found to be linearly related to the number of voltammetric cycles (similar results are found with films deposited without template). Beyond $1d$, it has not been possible to establish the relationship between cycle number and film thickness as the latter becomes difficult to measure. Furthermore an evaluation of the thickness deposited from the charge passed and account of the interstitial volume within the template necessitates measuring the density of the deposit as the porosity of the material is reported to produce significant differences between the density of bulk IrOx, *circa* 11 g cm^{-3} , and that of electrodeposited films *circa* 2 g cm^{-3} .²³ Characterisation with X-ray diffraction only produced a spectrum for the underlying gold substrate. However Raman microscopy clearly showed that the material was amorphous as deposited but became crystalline after annealing at 460°C .

Angle resolved reflectivity spectra of structured and non-structured IrOx films ($\frac{1}{2}d$ thick), Fig. 4, clearly demonstrates that, as with gold films,³³ the presence of the nanostructure imparts new optical properties to the material. In the case of the flat film, Fig. 4A, the reflectivity spectrum (normalized to the reflectivity from an aluminium mirror) changes in intensity with angle of incidence but does not change in wavelength or shape. In contrast, Fig. 4B, for the structured film there is a clear change in the position of the minimum reflectivity with angle. Two plasmon bands are observed in the data, Bragg diffracted by the

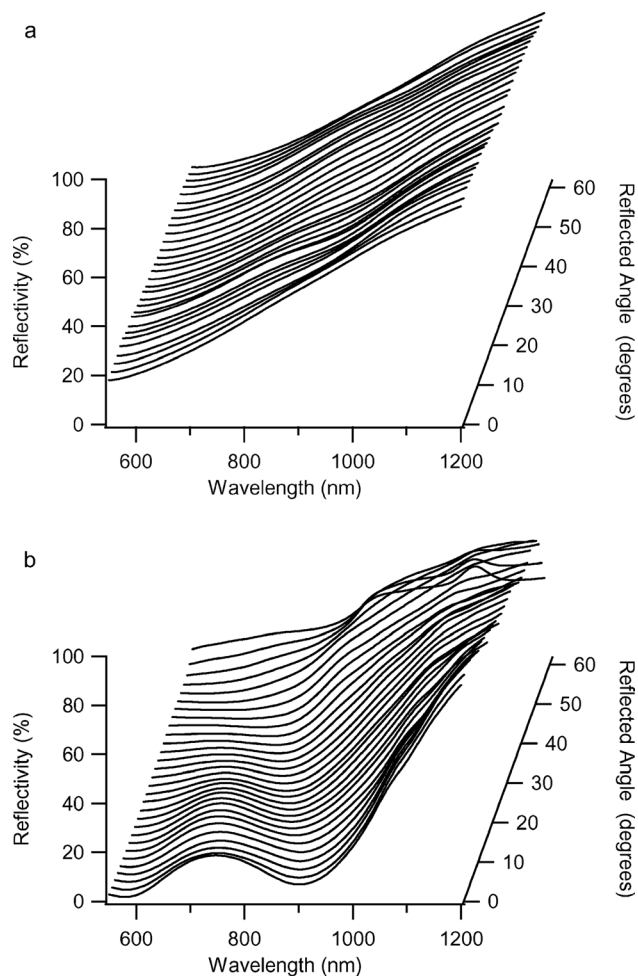


Fig. 4 Normalized reflectivity spectra recorded on (A) a non-structured film and (B) a structured film supporting plasmon, $\sim \frac{1}{2}d$, in air but with the films taken out of the solution in the bleached state.

periodicity of the dishes into the plane of the surface. The dispersion of these modes is governed by the high refractive index IrOx layer and the size of the dishes d . Initially coupled at 0° incidence, these modes tune to shorter wavelengths with increasing incident angles, indicative of delocalized behavior. Electrochromism was also observed when reflectivity spectra were recorded under potentiostatic control. For example, the intensity reflected at 770 nm varied from 100% at -0.3 V (the bleached state) to 67% at 0 V , 34% at $+0.1 \text{ V}$, 21% at $+0.2 \text{ V}$ and 16% at $+0.7 \text{ V}$ (the dark state). Detailed results recorded under potentiostatic control for different thicknesses will be reported subsequently.

Conclusions

This article reports the first successful preparation of highly ordered iridium oxide films *via* electrodeposition through a self-assembled colloidal template of polystyrene spheres. The films are true casts of the template; monolayer films present a long range hexagonal arrangement of hemispherical cavities while multilayer films present a 3D honeycomb structure with spherical voids characteristic of inverse opal structures. This approach avoids the

shrinkage normally observed with chemical and thermal transformations. The films are found to be amorphous, to have several electroactive redox states and to be electrochromic. Compared to flat films the reflectivity of the structured films is found to depend on the angle of incidence and wavelength of the incident light. These preliminary optical results suggest that nanostructured IrOx films could be used as electrochemically or chemically (IrOx is pH sensitive) tunable photonic devices.

Acknowledgements

The financial support of the EPSRC (EP/C511786/1) and of the Dorothy Hodgkin Foundation are gratefully acknowledged.

References

- 1 G. Beni, J. L. Shay, S. Gottesfeld and J. D. E. McIntyre, *Appl. Phys. Lett.*, 1978, **33**, 208–210.
- 2 J. D. E. McIntyre, W. F. Peck and S. Nakahara, *J. Electrochem. Soc.*, 1980, **127**, 1264–1268.
- 3 R. D. Meyer, S. F. Cogan, T. H. Nguyen and R. D. Rauh, *IEEE Trans. Rehab. Eng.*, 2001, **9**, 2–11.
- 4 S. C. Mailley, M. Hyland, P. Mailley, J. M. McLaughlin and E. T. McAdams, *Mater. Sci. Eng., C: Biomimetic and Supramolecular Systems*, 2002, **21**, 167–175.
- 5 D. O. Wipf, F. Y. Ge, T. W. Spaine and J. E. Bauer, *Anal. Chem.*, 2000, **72**, 4921–4927.
- 6 K. G. Kreider, M. J. Tarlov and J. P. Cline, *Sens. Actuators, B: Chem.*, 1995, **B28**, 167–172.
- 7 I. A. Ges, B. L. Ivanov, D. K. Schaffer, E. A. Lima, A. A. Werdich and F. J. Baudenbacher, *Biosens. Bioelectron.*, 2005, **21**, 248–256.
- 8 T. Pauporte, F. Andolfatto and R. Durand, *Electrochim. Acta*, 1999, **45**, 431–439.
- 9 R. S. Chen, Y. S. Huang, Y. M. Liang, D. S. Tsai and K. K. Tiong, *J. Alloys Compd.*, 2004, **383**, 273–276.
- 10 F. Y. Zhang, R. Barrowcliff, G. Stecker, W. Pan, D. L. Wang and S. T. Hsu, *Jpn. J. Appl. Phys., Part 2: Lett. Express Lett.*, 2005, **44**, L398–L401.
- 11 R. S. Chen, A. Korotcov, Y. S. Huang and D. S. Tsai, *Nanotechnology*, 2006, **17**, R67–R87.
- 12 A. Korotcov, Y. S. Huang, D. S. Tsai and K. K. Tiong, *J. Phys.: Condens. Matter*, 2006, **18**, 1121–1136.
- 13 A. M. Serventi, M. A. El Khakani, R. G. Saint-Jacques and D. G. Rickerby, *J. Mater. Res.*, 2001, **16**, 2336–2342.
- 14 Y. L. Chen, C. C. Hsu, Y. H. Song, Y. Chi, A. J. Carty, S. M. Peng and G. H. Lee, *Chem. Vap. Deposition*, 2006, **12**, 442–447.
- 15 P. N. Bartlett, J. J. Baumberg, S. Coyle and M. E. Abdelsalam, *Faraday Discuss.*, 2004, **125**, 117–132.
- 16 K. Yamanaka, *Jpn. J. Appl. Phys., Part 1: Regular Papers Short Notes & Review Papers*, 1989, **28**, 632–637.
- 17 M. C. Netti, M. D. B. Charlton, G. J. Parker and J. J. Baumberg, *Appl. Phys. Lett.*, 2000, **76**, 991–993.
- 18 M. Huppaufl and B. Lengeler, *J. Electrochem. Soc.*, 1993, **140**, 598–602.
- 19 M. Wang, S. Yao and M. Madou, *Sens. Actuators, B: Chem.*, 2002, **81**, 313–315.
- 20 C. Mousty, G. Foti, C. Comninellis and V. Reid, *Electrochim. Acta*, 1999, **45**, 451–456.
- 21 L. M. Schiavone, W. C. Dautremontsmith, G. Beni and J. L. Shay, *Appl. Phys. Lett.*, 1979, **35**, 823–825.
- 22 J. Yano, K. Noguchi, S. Yamasaki and S. Yamazaki, *Electrochem. Commun.*, 2004, **6**, 110–114.
- 23 M. A. Petit and V. Plichon, *J. Electroanal. Chem.*, 1998, **444**, 247–252.
- 24 G. S. Attard, P. N. Bartlett, N. R. B. Coleman, J. M. Elliott, J. R. Owen and J. H. Wang, *Science*, 1997, **278**, 838–840.
- 25 P. N. Bartlett, P. R. Birkin and M. A. Ghanem, *Chem. Commun.*, 2000, 1671–1672.
- 26 P. N. Bartlett, P. R. Birkin, M. A. Ghanem and C. S. Toh, *J. Mater. Chem.*, 2001, **11**, 849–853.
- 27 S. A. G. Evans, J. M. Elliott, L. M. Andrews, P. N. Bartlett, P. J. Doyle and G. Denuault, *Anal. Chem.*, 2002, **74**, 1322–1326.
- 28 T. Imokawa, K.-J. Williams and G. Denuault, *Anal. Chem.*, 2006, **78**, 265–271.
- 29 T. A. Kelf, Y. Sugawara, J. J. Baumberg, M. Abdelsalam and P. N. Bartlett, *Phys. Rev. Lett.*, 2005, 95.
- 30 G. V. Prakash, L. Besombes, T. Kelf, J. J. Baumberg, P. N. Bartlett and M. E. Abdelsalam, *Opt. Lett.*, 2004, **29**, 1500–1502.
- 31 S. Coyle, G. V. Prakash, J. J. Baumberg, M. Abdelsalam and P. N. Bartlett, *Appl. Phys. Lett.*, 2003, **83**, 767–769.
- 32 S. Coyle, M. C. Netti, J. J. Baumberg, M. A. Ghanem, P. R. Birkin, P. N. Bartlett and D. M. Whittaker, *Phys. Rev. Lett.*, 2001, 8717.
- 33 M. C. Netti, S. Coyle, J. J. Baumberg, M. A. Ghanem, P. R. Birkin, P. N. Bartlett and D. M. Whittaker, *Adv. Mater.*, 2001, **13**, 1368–1370.
- 34 S. Cintra, M. E. Abdelsalam, P. N. Bartlett, J. J. Baumberg, T. A. Kelf, Y. Sugawara and A. E. Russell, *Faraday Discuss.*, 2006, **132**, 191–199.
- 35 M. E. Abdelsalam, P. N. Bartlett, J. J. Baumberg, S. Cintra, T. A. Kelf and A. E. Russell, *Electrochem. Commun.*, 2005, **7**, 740–744.
- 36 M. E. Abdelsalam, P. N. Bartlett, T. Kelf and J. Baumberg, *Langmuir*, 2005, **21**, 1753–1757.
- 37 A. A. Zhukov, M. A. Ghanem, A. Goncharov, P. A. J. de Groot, I. S. El-Hallag, P. N. Bartlett, R. Boardman and H. Fangohr, *J. Magn. Magn. Mater.*, 2004, **272–276**, 1621–1622.
- 38 P. N. Bartlett, M. A. Ghanem, I. S. El-Hallag, P. de Groot and A. Zhukov, *J. Mater. Chem.*, 2003, **13**, 2596–2602.
- 39 N. D. Denkov, O. D. Velev, P. A. Kralchevsky, I. B. Ivanov, H. Yoshimura and K. Nagayama, *Langmuir*, 1992, **8**, 3183–3190.
- 40 M. Kawasaki, T. Sato and T. Yoshimoto, *Langmuir*, 2000, **16**, 5409–5417.
- 41 B. H. Juarez, C. Lopez and C. Alonso, *J. Phys. Chem. B*, 2004, **108**, 16708–16712.
- 42 J. Wijnhoven, S. J. M. Zevenhuizen, M. A. Hendriks, D. Vanmaekelbergh, J. J. Kelly and W. L. Vos, *Adv. Mater.*, 2000, **12**, 888–890.
- 43 P. V. Braun and P. Wiltzius, *Nature*, 1999, **402**, 603–604.
- 44 T. Sumida, Y. Wada, T. Kitamura and S. Yanagida, *Chem. Commun.*, 2000, 1613–1614.
- 45 T. Sumida, Y. Wada, T. Kitamura and S. Yanagida, *Chem. Lett.*, 2001, 38–39.
- 46 T. Sumida, Y. Wada, T. Kitamura and S. Yanagida, *Chem. Lett.*, 2002, 180–181.
- 47 P. N. Bartlett, T. Dunford and M. A. Ghanem, *J. Mater. Chem.*, 2002, **12**, 3130–3135.
- 48 L. D. Burke and R. A. Scannell, *Platinum Met. Rev.*, 1984, **28**, 56–61.